Title: Co-infection with *Leptomonas seymouri* enhances macrophage survival and promotes intracellular parasite persistence during *Leishmania donovani* infection

Sayantan Das[1¶], Pritam Dey Sarkar[1,2¶], Subhajit Biswas[*1,2]

Running head: *Leptomonas seymouri* can infect mammalian macrophages

Affiliations:

1. Infectious Diseases and Immunology Division, CSIR-Indian Institute of Chemical Biology, West Bengal, India.

2. Academy of Scientific and Innovative Research (AcSIR), Ghaziabad-201002, India.

[¶] S.D.and P.D.S contributed equally to this work.

*** Correspondence:** Subhajit Biswas

Email: subhajit.biswas@iicb.res.in; subhabiscam@gmail.com

ORCID Id: orcid.org/0000-0002-9001-7150

Abstract

Background

Leishmania donovani (LD) is an obligate intracellular parasite that survives and replicates within macrophages. *Leptomonas seymouri* (LS), a traditionally monoxenous trypanosomatid, has been repeatedly co-isolated with LD from visceral leishmaniasis (VL) and post-kala-azar dermal leishmaniasis (PKDL) patients in India, often together with *Leptomonas seymouri* narna-like virus 1 (Lepsey NLV1). Whether LS can survive and replicate within mammalian macrophages, and how co-infection influences parasite and viral dynamics, remains unresolved.

Methods and Findings

Using murine (RAW 264.7) and human (THP-1) macrophages, we systematically evaluated intracellular survival, replication, and revival of LS alone and during co-infection with LD. Quantitative ITS1 PCR demonstrated significant increases in intracellular parasite DNA over 48-168 h post-infection, with mean intracellular loads rising up to ~7.6-fold, indicating active replication rather than persistence. Reduced extracellular parasite load suggested restricted cell lysis and enhanced macrophage survival in co-infection compared to mono-infections. In co-infection scenario, generally LS displayed higher persistence compared to LD. Giemsa staining confirmed intracellular localization of LS. Parasites recovered from infected macrophages remained viable and revived as motile promastigotes, whereas extracellular parasites failed to survive beyond 48 h, confirming macrophages as the exclusive niche for prolonged viability. Interestingly, co-infection dampened macrophage IL-12 production, suggesting altered host immune activation. Lepsey NLV1 RNA accumulated predominantly within macrophages and

persisted up to 168 h post-infection. Virus load within LS in co-infection state was ~2.5-4 and ~7.5-23 fold higher (for RAW 264.7 and THP-1 respectively) compared to LS mono-infection. Purified virus alone failed to enter macrophages, indicating LS-dependent viral delivery.

Conclusions

Our findings question the prevailing view of LS as a strictly non-infective parasite, demonstrating its capacity to replicate within mammalian macrophages and persist during mono- or LD co-infection. The identification of a stable LD-LS-virus interaction highlights a previously underappreciated "triple-pathogen" biology with potential implications for VL and PKDL pathogenesis.

Keywords: *Leptomonas seymouri, Leishmania donovani,* Lepsey NLV1, Co-infection, Triple-pathogen, Visceral leishmaniasis.

1. Introduction:

Leishmania parasites are obligate intracellular pathogens that rely on macrophages for their survival, replication, and differentiation **[1].** Despite the extreme challenges posed by the intracellular environment, *Leishmania* are among the few protozoa capable of surviving and multiplying under such harsh conditions [2]**.** *Leptomonas seymouri* (*L. seymouri*; LS), typically a monoxenous trypanosomatid that infects insects, is generally not capable of infecting humans [3]**.** However, several reports from India indicated that this parasite could co-infect humans alongside *Leishmania donovani* (*L. donovani*; LD) in cases of visceral leishmaniasis (VL), cutaneous leishmaniasis and post-kala-azar dermal leishmaniasis (PKDL) [3–6]**.**

63 An in-depth study had been previously conducted to evaluate the infective potential of LS. It was
64 reported that despite several genetic adaptations, LS remained primarily a monoxenous organism
65 and couldn't infect mammalian macrophages such as J774 or BMMϕ, either on its own or
66 alongside LD [7]**.** Others implicated that it might infect mammals under specific conditions, for
67 instance, when the host's immune system was compromised by another pathogen such as LD or
68 HIV [6]**.** Interestingly, a study published in 1981 examined the interactions between LD and
69 *Leptomonas costoris* within peritoneal macrophages from hamster. It was observed that LD
70 differentiated into amastigotes and survived within cultured macrophages, whereas *L. costoris*
71 also differentiated into amastigotes but failed to survive. Additionally, macrophage cultures
72 infected with the infectious strain of LD retained 50% more *L. costoris* compared to control
73 macrophages that were infected solely with *L. costoris* [8]**.**

74 Macrophages serve as both the primary niche for *Leishmania* survival and replication, and as a
75 key effector population in parasite clearance [9]. However, the cellular consequences of LS
76 infection on macrophages remained largely unexplored, highlighting a critical knowledge gap
77 that warranted systematic investigation.

78 The presence of *Leishmania* RNA virus (LRV) is known to enhance the persistence and worsen
79 the pathogenesis of *Leishmania sp*.[10,11]**.** Unexpectedly, LS was found to harbour a distinct
80 protozoan virus, *Leptomonas seymouri* narna-like virus 1 (Lepsey NLV1), an RNA virus of
81 approximately 4.5 kb **[12].** A study from India reported that >90% of LD laboratory isolates
82 from clinical samples of VL were co-infected with LS. Lepsey NLV 1 was predominantly
83 present in the LS-positive samples (75% of the laboratory isolates) [13]**.** Recent findings reported
84 that LS and Lepsey NLV1 could be even detected alongside LD in archived serum samples of
85 kala-azar or PKDL patients. It also suggested that Lepsey NLV1 might enhance the persistence

86 of LD and dampen immune responses by down-regulating IL-18 [14] ,which also corroborated
87 with the results from a previously published LRV2+ *L. major* study [15]**.** Leishmania RNA
88 viruses (LRVs) had been known to exacerbate *Leishmania* pathogenesis. In comparison, whether
89 or not Lepsey NLV1 is linked to pathogenesis or persistence of VL/PKDL ("triple pathogen
90 phenomenon") warrants further investigation.

91

92 2. MATERIALS AND METHODS:

93 2.1. Parasite culture:

94 *Leishmania donovani* (MHOM/IN/1983/AG83) and *Leptomonas seymouri* (ATCC)
95 promastigotes were cultured at 22 °C in M199 (Sigma) with 10% heat-inactivated fetal bovine
96 serum (FBS) (Gibco) and 1% L glutamine-penicillin-streptomycin solution (Sigma).
97 Promastigotes were harvested on the 6th or 7th day of the stationary phase of growth for *in vitro*
98 infection.

99 2.2. Murine macrophage culture:

100 Murine macrophage cell line RAW 264.7 was cultured at 37 °C with 5% CO_2 in DMEM
101 (Dulbecco 's modified Eagle's medium) supplemented with 10% heat-inactivated fetal bovine
102 serum (FBS) (Gibco) and 1% L glutamine-penicillin-streptomycin solution (Sigma).

103 For infection experiments, cells were plated in a 12-well flat bottom plates (Nunclon Delta
104 Surface^{TM}, Thermo scientific) with $2x10^5$ cells and incubated at 37 °C with 5% CO_2 for 48h.
105 Cells were counted at $8x10^5$/well at 80% confluency.

106 ## 2.3. Human monocyte culture:

107 Human monocyte cell line THP-1 was cultured at 37 °C with 5% CO_2 in RPMI medium
108 supplemented with 10% heat-inactivated fetal bovine serum (FBS) (Gibco) and 1% L glutamine-
109 penicillin-streptomycin solution (Sigma).

110 ## 2.4. THP-1 activation:

111 For infection experiments, cells were plated in a 6-well flat bottom plates (Nunclon Delta
112 Surface™, Thermo scientific) with $5x10^5$ cells /well. Before infection, cells were stimulated with
113 100 nM /well of 4α-phorbol 12-myristate 13-acetate (PMA) (Sigma, USA) to induce
114 differentiation into macrophage-like cells. The cultures were then incubated for 24 h at 37 °C in
115 a humidified atmosphere containing 5% CO_2. Following differentiation, wells were gently
116 washed twice with culture medium (without PMA) to remove any non-adherent cells.

117 ## 2.5. *In vitro* infection:

118 Accordingly, macrophages were infected with 10^7 stationary phase promastigotes of *Leishmania*
119 *donovani* (AG83), *Leptomonas seymouri* (ATCC) and 10:1 Co-culture (LD: LS) at a MOI of
120 10:1 (parasite: MQ ratio) and incubated at 37C with 5% CO_2 for 4 hours. Cells were then washed
121 twice with media to remove non-adherent parasites and incubated with media for 48 hours to 168
122 hours. After the post-infection incubation period, the cells were processed for further analysis.

123

124

2.6. Extraction of purified Lepsey NLV1 and *in vitro* infection with virus:

For extraction of purified Lepsey NLV1 virus, approx. 10^8 LS parasites were frozen at –80 °C for 3 hours, followed by thawing at 37 °C. Sonication was performed using three pulses of 10 seconds each. The samples were then centrifuged at 3000 rpm for 10 minutes to pellet down the *Leptomonas seymouri* (LS) cells. The resulting supernatant, containing the Narna-like virus 1 (NLV1), was collected, passed through a 0.22 µm syringe filter to remove residual cellular debris, and stored as 500 µl aliquots for downstream applications.

For *in vitro* infection, RAW 264.7 macrophage cells were infected with purified Lepsey NLV1 at a MOI =10 and incubated at 37C with 5% CO_2 for 4 hours. After 4 hours, the inoculum was not removed and supplemented with DMEM-1% FBS for further incubation. After 48, 72 and 96 h.p.i., cell supernatants and lysates were collected for further assays.

2.7. Macrophage infected parasite revival assay:

To check the if the parasites are viable and can revive from infected macrophages, 10^6 RAW 264.7 macrophages were infected with only LD, LS or a 2:1 and 10:1 (LD:LS) Co-culture at a MOI of 1:10. After 4 hours of infection, non-adhered parasites were removed by twice washing the cells twice with 1X PBS. Cells were maintained in DMEM-10 at 37C with 5% CO2 for 48 to 168 hours. After every incubation period, the sup was collected and 500 ul cell lysates (in DMEM-10) were added to 5 ml Scneiders medium with 20% FBS and incubated at 22°C and incubated for at least 48 hours to check the transformation of parasites from infected macrophages.

146 To exclude any possibility of parasite viability in DMEM10, 10^7 parasites /well were maintained
147 in DMEM-10 at 37 °C for 48-168h and subsequently 2 x 10^6 parasites/time point were
148 transferred to Schneider's medium at 22 °C to assess revival capacity at different time points.
149 Parasite titre was quantified 9 days post inoculation in Schneider's media using ITS1 qPCR. In
150 another set of experiment, 10^6 viable LS parasites /well were inoculated into 12-well plates and
151 incubated at 37°C in DMEM-10 for 8 days. For further verification, 10^6 LD and 10^6 LS parasites
152 were cultured in both DMEM-10 and RPMI-10 at 37°C for a period of 24, 72- and 168-hour time
153 points. Both microscopic and molecular analysis (ITS1 PCR) were performed to check the
154 replication of parasites. Parasite titre was determined from densitometric analysis of specific
155 bands on gel using ImageJ software.

156 2.8. DNA extraction and ITS1 gene PCR:

157 DNA was extracted from 200 ul of parasite infected cell supernatant or cell lysate using a
158 QIAamp DNA Mini kit (Qiagen The quality and concentration of DNA was assessed using a
159 NanoDrop spectrophotometer (Thermo Scientific, USA).

160 An rDNA-ITS1 fragment was directly amplified from the isolated DNA using ITS1-FP (5'
161 CTGGATCATTTTCCGATG 3') and ITS1-RP (5' TGATACCACTTATCGCACTT 3') primers.
162 The PCR protocol included an initial denaturation at 94°C for 10 minutes, followed by 40 cycles
163 consisting of denaturation at 94°C for 1 minute, annealing at 54°C for 1 minute, and extension at
164 72°C for 1 minute. A final elongation step was performed at 72°C for 10 minutes. PCR products
165 were analysed using 1.0% agarose gel containing SYBR safe for nucleic acid staining. DNA
166 from the *Leishmania donovani* strain MHOM/IN/1983/AG83 (320 bp) and *Leptomonas seymouri*
167 (ATCC) (418 bp) was used as a positive control, while nuclease-free water served as the non-

168 template control (NTC). For *L. seymouri* specific PCR, primers and conditions were followed as
169 described previously (13).

170 2.9. Real Time PCR and Image J Analysis:

171 A quantitative real-time PCR assay was designed to quantify the parasite DNA copy number in
172 the samples using a SYBR Green dye-based quantitative (q)PCR with the Luna Universal PCR
173 reagent (New England Biolabs). Equal amounts of DNA from each experimental condition were
174 used for qPCR analysis. A 320 bp and 418 bp fragment of the ITS-1 gene was amplified using
175 the same primers as previously described (Table 1). The reactions were carried out on a
176 StepOne™ system (Applied Biosystems, Thermo).

177 The presence of bands of the expected size was further verified through 1% agarose gel
178 electrophoresis of qPCR products. To determine the LD:LS ratio in Co-infected samples, specific
179 bands (both standard and samples) from digital images of the gel were subjected to densitometric
180 analysis using ImageJ software.

181 2.10. RNA Extraction and cDNA synthesis:

182 Total RNA was extracted from infected macrophage cell supernatant or cell lysates using
183 standard TRIzol method following manufacturer's kit protocol (PureLink RNA Minikit,
184 Invitrogen). For detecting virus load in vivo, total RNA was extracted similarly from whole
185 blood (100-200 ul), urine (100 ul) and Splenic tissue cultures (500 ul). RNA from spleen and
186 liver tissue was isolated using RNeasy Kit (Qiagen). The concentration and purity of RNA was
187 determined using a Nanodrop One spectrophotometer (Thermo Scientific, USA).

188 The extracted RNA was subjected to cDNA synthesis and virus specific nested PCR using
189 primers and protocol as previously described in (14). PCR products were separated using 1%
190 agarose gel electrophoresis. Bands of the expected size were either gel-purified using the
191 QIAGEN Gel Extraction Kit (Germany) or PCR-purified using the QIAGEN PCR Purification
192 Kit (Germany) before DNA sequencing.

193 2.11. Real Time PCR:

194 The viral RNA copy number in the nucleic acid isolated from the samples were ascertained using
195 qRT-PCR. The primers CT2-F and CT2-R were used to amplify a 338 bp segment of the Lepsey
196 NLV1 gene using protocol as described elsewhere [14]. Specific amplified products were
197 visualized in 1% agarose gel electrophoresis with SYBRsafe™ for nucleic acid staining.

198 2.12. Giemsa Staining:

199 Cells were plated in a 4-well chamber (Genetix Biotech) tissue culture slide with $5x10^4$ cells
200 (RAW 264.7) or 10^5 (THP-1) and incubated at 37 °C with 5% CO2 overnight. Macrophages
201 were infected with the stationary phase of *Leishmania donovani* (AG83), *Leptomonas seymouri*
202 (ATCC) or 10:1 Co-culture (LD:LS) promastigotes at a MOI of 10:1 (parasite: MQ ratio) and
203 incubated at 37C with 5% CO_2 for 4 hours. Cells were then washed twice with media to remove
204 non-adherent parasites and incubated with media for 72 hours. After the incubation period, cells
205 were fixed with methanol and stained with Giemsa. The stained slides were visualized under an
206 optical microscope (EVOS microscope) for determining the infection of macrophages at 1000x
207 magnification.

208

209 ## 2.13. IL-12 (p40) ELISA:

210 Quantitative IL-12 p40 ELISA (BD OptEIA™, Cat. No.- 555165) was performed as per
211 manufacturer's protocol to determine cytokine levels from cell supernatants of infected RAW
212 264.7 cells at 72 h.p.i. Standard curve was prepared using dilutions of the respective recombinant
213 cytokine provided with the kit.

214 ## 2.14. Statistical Analysis:

215 Statistical analysis was performed using GraphPad Prism version 8.0 (GraphPad Software,
216 USA). Data are expressed as mean ± SD unless otherwise indicated. Statistical tests were
217 selected based on experimental design and data distribution. Differences between two groups
218 were evaluated using unpaired two-tailed Student's t-test. For comparisons involving more than
219 two groups, one-way ANOVA followed by Tukey's post hoc test was used. Each experiment
220 was performed using at least three independent biological replicates. A p value of < 0.05 was
221 considered statistically significant. Exact p values are reported where applicable.

222

223 # 3. RESULTS:

224 ## 3.1. Monoxenous parasite *Leptomonas seymouri* harbouring Lepsey
225 ## NLV1 could efficiently infect and replicate in mammalian
226 ## macrophage cells

227

228 ### 3.1.1. LD-LS co-infection led to ~300-2500-fold higher extracellular *L.*
229 ***seymouri* load compared to *L. donovani***

230 ITS-1 PCR–based quantification revealed that extracellular parasite DNA from LD, LS, and co-
231 culture (2:1) infected RAW 264.7 macrophage cells showed a modest, non-significant (~1.6-
232 fold) rise between 48 and 168 h.p.i. Only 10:1 co-culture demonstrated a significant (~2.9-fold)
233 increase (Fig 1A). The mean intracellular (IC) DNA levels significantly increased ~7.6-fold over
234 the same period, indicating sustained replication within macrophages (Fig 1B). Total parasite
235 DNA count (LD, LS, co-cultures 2:1 and 10:1) inside macrophages (IC) increased by
236 approximately 1.1 and 5.0-fold, compared to total parasite DNA in supernatant (EC) at 48- and
237 168 h.p.i. respectively. The mean combined parasite load (EC+IC) at 168 h.p.i. increased ~4.7-
238 fold compared to 48 h.p.i. These data supported active proliferation rather than persistence of LS
239 inside macrophages alone or when present with LD over 168 hours. The ~2-fold rise in IC LS
240 DNA at 168 h.p.i. compared to the initial inoculum (10^7 LS; though two-times washed after 4 h
241 of cellular internalization) confirmed true intracellular replication rather than residual carry-over
242 (S1 Table). ImageJ-based band intensity and standard-curve analysis further demonstrated that
243 LS replicated far more efficiently thereby rupturing and getting released in the extracellular
244 milieu at higher proportions up to $2x10^3$-fold at 48 h and $2.5x10^3$-fold at 168 h compared to LD
245 in co-culture infected cells. Despite higher initial LD abundance (2:1 or 10:1), the IC LD: LS
246 ratio stabilized at ~1:150 to 1:66 at 48- and 168 h.p.i time points respectively. Interestingly, the
247 EC ratio shifted from 1:333 to 1:2500, suggesting rapid and more pronounced lysis of LS-
248 infected macrophage cells. (S2 Table).
249

250 ### 3.1.2. Temporal quantification revealed differential replication and
251 population dynamics of LD and LS in co-infected human macrophages

252 Similar to findings in murine macrophages, both LD and LS successfully infected and replicated
253 within differentiated human monocyte–derived macrophages (THP-1). The mean extracellular
254 (EC) parasite DNA count (LD, LS and co-culture 10:1) increased by ~1.17 fold and ~1.71- fold
255 at 96 and 168 h.p.i, respectively compared to 48 h.p.i (Fig 1C). The mean intracellular (IC)
256 parasite DNA levels increased significantly by approximately 1.77 and 4.3-fold at 96 and 168
257 h.p.i compared to 48 h.p.i (Fig 1D). The mean parasite DNA count (LD, LS and co-culture 10:1)
258 inside macrophages (IC) increased by approximately 1.76, 2.66 and 4.46-fold, compared to mean
259 parasite DNA in supernatant (EC) at 48, 96 and 168 h.p.i. respectively. Combined parasite load
260 (EC+IC) increased by approximately 1.55 and 3.37-fold at 96 and 168 h.p.i compared to the
261 initial time point of 48 h.p.i. These results further validated the replication of monoxenous
262 parasite LS inside mammalian macrophages (S3 Table). Image J analysis of the relative ITS-1
263 PCR products revealed that in case of co-culture, LD load was more than LS in supernatant at 48
264 h.p.i. However, this scenario was reversed at 96 and 168 h.p.i. Inside macrophages (IC), the LD:
265 LS DNA ratio was 67:1 at 48 h.p.i, which decreased to 1:1.3 at 168 h.p.i. Interestingly, the LD:
266 LS ratio in supernatant (EC) reversed from 2.5:1 at 48 h to 1:50 at 168 h.p.i. This suggested that
267 the LS parasites were released rapidly from macrophages at later time points (upon infected cell
268 lysis) which resulted in greater to at least equal LD: LS ratio inside macrophages from 48- to 168
269 h time points respectively (S4 Table).
270

3.2. Macrophage internalized parasites transformed to promastigotes when cultured in Schneider's medium

3.2.1. Parasites remained viable after infecting murine macrophage cells RAW 264.7

For every time point yield (72–168 h), transformation of amastigotes to promastigotes (reactivation) was carried out in sub-culture flasks containing supplemented Schneider's Drosophila medium. These subcultures were examined at 48 h post-transfer under the microscope to check for any viable and motile parasites i.e. transformed promastigotes. Four representative microscopic fields were observed per flask and motile cells were enumerated (Data in S5 Text). Sub-cultures were further incubated, and two representative fields were observed per flask again at 11 days p.i. (Data in S6 Text)

The 48 h counts upon transfer from each time-point harvest showed that the number of parasites increased progressively in the sub-culture flasks from earlier to later time-point harvests, indicating increasing amastigote production within macrophages over 7 days. Increased parasite counts at 11 days p.i. in the subculture flasks compared to corresponding 48 h counts indicated successful replication of transformed promastigotes upon revival of amastigotes in supplemented Schneider's Drosophila medium. For instance, LS subculture from the 120-h original harvest showed an increase in parasite count between early (2 days post subculture) and later observations (11 days subculture), confirming parasite viability and proliferation in Schneider's medium. At 12 days p.i., viable, motile cells in the total subcultures were also quantified using a haemocytometer (Fig 1E and S7 Table), supporting the microscopic counts.

292 To compare the intrinsic growth properties of the revived parasites, 10^6 viable parasites from the
293 12th day harvest of the subculture flasks was further cultured and monitored up to 168 h in
294 Schneider's medium. Haemocytometer counts showed that LS-containing cultures (alone or in
295 mixtures) grew to higher titres at 96 h and 168 h compared to LD-only cultures (Data in S8
296 Text).

297 Importantly, additional observations revealed that adhered, non-phagocytosed parasites could
298 remain static but viable in DMEM-10 up to 48 h during macrophage infection, and when
299 transferred to Schneider's medium they regained the capacity to proliferate. However, such
300 revival did not occur in case of later harvests of infected macrophages (>48 h). Non-internalised
301 parasites could neither persist beyond 48 h in DMEM-10, nor regained viability when transferred
302 to Schneider's medium at 22 °C (Fig 1F). This clarified that any apparent revival beyond 48 h
303 observed in Schneider's medium, was only from intracellular amastigotes that transformed in the
304 subculture flasks.

305

306 **3.2.2. LD or LS could not replicate to higher titres in DMEM-10 or RPMI-10**
307 **at 37°C**

308 In order to test whether free parasites could replicate in macrophage culture conditions, viable
309 LS parasites were inoculated into 12-well plates at 10^6/well and incubated at 37°C in DMEM and
310 RPMI-1640 supplemented with 10% FBS for 7 days. No motile or viable parasites were
311 observed at the end of the experiment.

312 It was further evident from both molecular analysis (PCRs) as well as microscopic analysis
313 neither LD nor LS could not grow in DMEM-10 or RPMI-10 at 37°C when tested over a time

314 point of 168 h. The titre was estimated (IMAGE J analysis) to stay around 10^4-10^5 parasites per
315 5ml (10^4 for LD and 10^5 for LS) culture over a period of 24-168 h post-inoculation in the
316 aforesaid growth media (Fig 1G).

317 As mentioned earlier, LS stayed static but viable up to 48 h but then became non-viable and
318 could not be revived beyond 48 h of culture. Hence, it can be concluded that LS detected in the
319 sub-cultures (in Schneider's medium at 22 °C) from macrophage-infected yields at 72h time
320 point onwards, must had replicated inside the macrophages and revived as promastigotes in the
321 subculture media.

322

323 3.3. IL-12 cytokine profiling reflected immune modulatory role of LD, LS and 324 co-infective states

325 IL-12 (p40) ELISA from 72 h supernatant of infected RAW 264.7 cells revealed that LD-
326 infected cells induced the highest IL-12 protein expression by approximately ~2.62-fold
327 compared to the uninfected control cells. LS-infected cells did not show any significant change
328 in IL-12 levels compared to LD-infected cells. In contrast, co-culture-infected cells showed
329 reduced IL-12 expression, approximately ~1.43-fold lower compared to LD-infected cells (Fig
330 1H). It may be an indication of dampened pro-inflammatory signalling, possibly linked to
331 reduced macrophage activation, higher parasite load, and prolonged persistence.

332

3.4. Lepsey NLV1 was detected more (10-100 times) inside mammalian macrophages compared to extracellular milieu

3.4.1. Intracellular persistence of Lepsey NLV1 without temporal proliferation in murine macrophages

RT-PCR analysis at 48 h.p.i. confirmed the presence of Lepsey NLV1 RNA within RAW 264.7 macrophages. Intracellular (IC) viral level was approximately ~20-130-fold higher than the extracellular (EC) fraction (Fig 2A). Lepsey NLV1 titre was further estimated from 48-168 h.p.i. in a time point assay. 14-fold greater viral load was detected in IC than EC at 48 h.p.i. IC viral titres were found to remain stable at 7.0–8.0 × 10^7 gE/well, whereas EC titres were maintained at lower levels (4.0–6.0 × 10^6 gE/well) (Figs 2B and 2C). Although, the total LS count decreased in co-infections as compared to the LS mono-infection, the total viral titre remained static in both the scenarios (S9 Table). Overall results suggested no progressive increase in virus titre inside the host macrophages over 7 days (168 h.p.i). LS carrying Lepsey NLV1 efficiently entered RAW 264.7 macrophages, confirming strong intracellular localization.

3.4.2. Human monocyte-derived macrophages supported progressive intracellular replication of Lepsey NLV1 unlike murine macrophages

Similar analysis confirmed the presence of Lepsey NLV1 RNA in differentiated human monocyte-derived macrophages (THP-1) at multiple post-infection time points. Extracellular (EC) titres in LS infection for Lepsey NLV1 declined modestly from 48 h.p.i. to 168 h.p.i by ~1.45-fold. Viral titre in co-culture 10:1 infected cell supernatant increased by ~1.36-fold from 48 h.p.i. to 96 h.p.i (Fig 2D). The mean intracellular (IC) titres in LS and co-culture infected

354 cells significantly increased from 48 h.p.i. to 96 h.p.i. and 168 h.p.i by ~4.33-fold and ~4.15-fold
355 respectively (Fig 2E). IC viral titre increased compared to EC levels by ~10.3-fold, ~46-fold and
356 ~57.6-fold at 48, 96 and 168 h.p.i., respectively, indicating strong intracellular retention. Total
357 viral load (EC + IC) increased over time and peaked at 96 h.p.i. ($1.74 \pm 0.53 \times 10^7$ gE), possibly
358 due to increase in total LS count over time from 48-168 h.p.i (S10 Table). These findings
359 showed that Lepsey NLV1 persisted at ~10 –100 -fold higher levels intracellularly than in the
360 extracellular environment.

361 3.4.3. Lepsey NLV1 extracted from LS, could not alone infect macrophage 362 cells

363 In contrast, purified Lepsey NLV1 (obtained by sonication, sedimentation and filtration of LS
364 cultures) failed to infect RAW 264.7 macrophages. Viral RNA was detected from 48 to 96 h.p.i.
365 It was limited to the supernatant and remained comparable to inoculum levels, with no
366 intracellular detection (Figs 2F and 2G). These findings indicated that purified Lepsey NLV1
367 alone could not enter or replicate in macrophages independently. Thereby, it highlights LS as a
368 necessary carrier, likely delivering the virus via phagocytosis of infected parasites rather than
369 direct cellular entry.

370

371 ## 3.5 Microscopic observation of mammalian macrophages infected
372 with *L. donovani* or *L. seymouri*

373 Spherical shaped amastigote images were observed under microscope at 72 h.p.i. inside Giemsa
374 stained macrophages. LS amastigotes were visible within both RAW 264.7 (Figs 3A-C) and
375 THP-1 cells (Figs 3D-F), albeit less conspicuously compared to LD.

376

377 # Discussion:

378 Here, we conducted a comprehensive assessment of the infectivity of LS, a parasite frequently
379 co-isolated with LD from kala-azar patients in India [13]. *In vitro* results from this study,
380 suggested that LS could infect murine as well human macrophage cells such as RAW 264.7 and
381 THP-1 respectively. Although the two parasites showed increased intracellular DNA over time,
382 LS was abundantly detected in intracellular (IC) and extracellular (EC) compartments, both
383 alone and as co-infecting parasite with LD. In co-infection scenario, upon progressive infection,
384 the markedly higher extracellular LS burden suggested efficient intracellular amastigote
385 replication coupled with enhanced LS-induced host-cell rupture, thereby increasing the
386 extracellular release of LS amastigotes. The 2-fold increase in LS DNA in IC compartment at
387 168 h.p.i. compared to the initial inoculum (10^7 LS; though two-times washed after 4 h of
388 cellular internalization) confirmed true intracellular replication of LS rather than residual carry-
389 over. Moreover, co-infection experiments revealed that the presence of LD did not adversely
390 affect LS replication. On the contrary, in murine macrophage cells, LS replicated faster

391 compared to LD resulting in 1:66 ratio in IC milieu at 168 h.p.i. despite 2 or 10-fold more
392 abundance of LD in the original inoculum (LD: LS=2:1 or 10:1). A comparable earlier study,
393 likewise, demonstrated critical preliminary evidence of the varying ability of LD strains to alter
394 macrophage function, notably impairing the digestion of subsequently internalized *Leptomonas*
395 sp and facilitating *Leptomonas* sp. survival [8]**.**

396 The THP-1 macrophage infection model further corroborated our observations in murine RAW
397 264.7 cells, confirming that LS could infect and replicate within differentiated human monocyte–
398 derived macrophages. Although both LD and LS showed increasing intracellular parasite DNA
399 over time, intracellular accumulation was greater than extracellular levels. Thus, suggesting
400 active intracellular replication of LS rather than extracellular release. Importantly, the increase in
401 combined parasite load (EC+IC) over time further supported active replication of LS within a
402 human macrophage environment, thereby extending our murine findings to a clinically relevant
403 host cell system.

404 In co-infection, a marked temporal shift in LD:LS ratio was observed. While LD predominated
405 in the supernatant at 48 h.p.i., LS became the dominant extracellular parasite at 96 and 168 h.p.i.,
406 coinciding with a sharp reduction in the intracellular LD:LS ratio. This reciprocal redistribution
407 suggested progressive intracellular accumulation of LS followed by enhanced release into the
408 extracellular milieu at later time points, likely associated with increased rupture of LS-infected
409 macrophages, consistent with observations in RAW 264.7 cells.

410 Interestingly, the intracellular persistence of LS in the presence of LD, as reflected by the
411 stabilization of LD: LS ratios within macrophages over time, suggested that co-infection did not
412 impose a competitive disadvantage on LS. Instead, LD might have provided a permissive

413 intracellular niche that supported LS survival and replication in human macrophages. This
414 phenomenon mirrored our murine macrophage findings and argued against the notion that LS
415 replication is typically restricted to insect hosts (Fig 4).

416 Our observations didn't align with a previous report that LS, as a monoxenous kinetoplastid,
417 could not be replicated in mammalian cells (although different macrophage cell lines, J774 and
418 BMMϕ were used) [6]. Taken together, the RAW 264.7 and THP-1 infection models collectively
419 supported a broader host adaptability of LS, highlighting its capacity for sustained intracellular
420 replication, enhanced cyto-pathogenicity, and efficient dissemination from mammalian
421 macrophages especially under co-infection conditions.

422 This is further consistent with earlier hypotheses that LS may act as a commensal or co-
423 endosymbiont in LD infections, potentially influencing disease outcomes [16]. The viability
424 assays demonstrated that parasites harvested from macrophage infections could be successfully
425 revived in serum-supplemented Schneider's medium across multiple time points (72h-168h),
426 confirming their persistence in intracellular environments. The progressive increase in parasite
427 counts during sub-culturing underscored that LS retained their proliferative potential post-
428 macrophage passage. However, the inability of free, non-internalised parasites to persist or
429 replicate in macrophage culture conditions indicated that parasite survival beyond 48 h was
430 exclusively attributable to an intracellular niche. Transfer of known number of parasites (3×10^6)
431 from macrophage culture media to Schneider's medium beyond 48 h up to 168 h post-
432 inoculation didn't result in any restoration of motility of parasites even after 9 days incubation
433 and the final yields came less than inoculum. Only static parasites at 48 h in macrophage media
434 gained motility and replicated in Schneider's growth medium. These observations ruled out

435 extracellular contamination as a confounding factor and strengthened the conclusion that parasite
436 revival from cultures beyond 72 h.p.i. represented genuine intracellular survival and release.
437 Conversely, neither LS nor LD parasites were able to replicate in DMEM-10 or RPMI-10 at
438 37°C media used during macrophage infections where parasite counts remained static and no
439 motile forms were detected up to 8 days post-inoculation.

440 These data convincingly ruled out extracellular replication in culture medium, implicating
441 intracellular macrophage environments as the primary niche for LS persistence and propagation
442 during infection, consistent with previous suggestion of LS adaptation under host-induced
443 selective pressures [5,16]**.** Taken together, these results emphasized the importance of the host
444 cellular environment in sustaining parasite viability and suggested that LS possessed enhanced
445 capacity to endure intracellular stress, a feature that might redefine its ecological persistence and
446 pathogenic potential.

447 Dampened IL-12 secretion upon co-infection compared to mono-infections suggested a possible
448 evasion mechanism from host immune system, consistent with the frequent detection of LD-LS
449 co-infection in clinical VL samples. These observations aligned with our previously published
450 observation of reduced IL-18 levels in human serum samples in case of co-infection cases
451 compared to LD only samples [14]. Taken together, these results emphasized the importance of
452 the host cellular environment in sustaining parasite viability. It suggested that LS possessed
453 enhanced capacity to endure intracellular stress, a feature that might redefine its ecological
454 persistence and pathogenic potential.

455 Microscopic evaluation of Giemsa-stained RAW 264.7 and THP-1 cells revealed amastigote-like
456 forms of both LD and LS at 72 h.p.i. LD-infected cells exhibited more distinct amastigote forms.

457 In contrast the presence of LS in intracellular compartments, albeit less prominently, suggested a
458 morphologically adaptive, possibly amastigote-like transformation of LS under intracellular
459 stress. Notably, these findings diverged from the results reported by Kraeva et al., possibly due
460 to differences in murine host cell lines employed, such as J774 or BMMϕ, which might not have
461 supported LS persistence [6]**.** The replication and persistence of LS in mammalian macrophage
462 cells further supported our molecular and growth-based observations of transient intracellular
463 survival.

464 This study substantiated that LS, carrying Lepsey NLV1, could enter and persist within
465 mammalian macrophages. RT-PCR revealed higher intracellular viral loads than extracellular
466 milieu at 48h.p.i. This indicated efficient LS uptake and potential viral retention or amplification
467 inside macrophages. Detected intracellular titres (10^6-10^7 gEs) contrasted with ~10^5-10^6 gEs in
468 supernatants. This indicated robust intracellular localisation. This pattern remained stable over
469 168 h in murine macrophages, implying a non-replicative or tightly controlled viral state inside
470 macrophage cells. The lack of increasing titre post-infection possibly reflected macrophage-
471 mediated restriction or a steady-state balance of replication and degradation. Interestingly, in
472 THP-1, a slight increase of ~4 fold in mean viral titre was observed in the tested time points
473 compared to the initial time point of 48 h.p.i. (in case of mono- or co-infection). In THP-1, the
474 reduction in total viral titre in the co-infection scenario compared to LS infection alone was
475 negligible (~1.6-6.5-fold). This decrease was minimal relative to the significant reduction in LS
476 parasite counts (~4-15-fold in EC versus ~50-1000-fold in IC) observed from 48 to 168 h.p.i.
477 Therefore, co-infection with LD possibly appeared to favor virus replication and persistence
478 within LS, although LS count was lower compared to only LS infection. The schematic
479 highlights enhanced viral replication and improved LS persistence in the presence of LD across

480 murine and human macrophage models. It was evident from our calculations that the parasite:
481 virus ratio in case of co-infection was significantly higher (2.5-23-fold) compared to LS mono-
482 infection in case of both types of macrophages tested (Fig 4). .

483 Notably, purified Lepsey NLV1 could not enter or replicate in macrophages independently,
484 thereby highlighting LS as a necessary carrier, likely delivering the virus via phagocytosis of
485 infected parasites rather than direct cellular entry. Recent LD cases in Himachal Pradesh reported
486 LS co-infection, raising questions about the virus's role in atypical cutaneous manifestations [3].
487 The exact impact of Lepsey NLV1 dynamics and host-pathogen interaction, however, remained
488 to be fully explored.

489 Taken together, our findings presented a thought-provoking re-evaluation of LS, particularly in
490 co-infection scenarios with LD. This study critically redefined the biological and pathogenic
491 profile of LS, challenging its long-held classification as a non-infective, monoxenous parasite,
492 but as a potentially replicative parasite capable of persisting within mammalian macrophages.
493 The association of LS with the Lepsey NLV1 virus introduced a significant paradigm shift,
494 highlighting a complex LD-LS-virus (triple pathogen) biology. It is noteworthy that *Leptomonas*
495 sp. had been previously associated with infections in immunosuppressed patients [17]. These
496 findings underscored the underestimated pathogenic potential of LS. It warrants a detailed
497 mechanistic study into host-pathogen dynamics and its influence on *Leishmania* disease
498 outcomes, particularly in co-infection contexts.

499

500

501

FUNDING

The research was funded by Indian Council of Medical Research; grant number: Discovery/IIRP/SG-0959/2023 (GAP-473). The grant was given to S.B. The funders had no role in the study design, analysis and interpretation of data; in the writing of the manuscript; and in the decision to submit the manuscript for publication.

AUTHORS' CONTRIBUTION

S.B., S.D. and P.D.S. conceived and designed the experiments. S.D. and P.D.S performed the experiments equally. S.D. and P.D.S. performed data analysis and S.B. performed critical analysis of the data. S.B. provided funding, reagents, materials and analysis tools. S.B., S.D. and P.D.S. jointly wrote the original draft of the manuscript. All authors critically reviewed and modified and agreed on the current version of the manuscript.

ACKNOWLEDGEMENT

Authors acknowledge the support received from the Director of CSIR-IICB. S.B. also acknowledges AcSIR for support. S.D. and P.D.S acknowledges the support of UGC for their UGC- Research Fellowships. The authors would also like to acknowledge the use of relevant facilities at CSIR-IICB including the Central Instrumentation Facility (CIF). The authors acknowledge CSIR-IICB for providing all laboratory facilities for conducting the current work.

DECLARATION OF INTEREST

The authors declare no competing interests.

522 # DATA AVAILABILITY

523 Further information and resource requests should be directed to and will be fulfilled by the
524 corresponding author, Dr. Subhajit Biswas (subhajit.biswas@iicb.res.in;
525 subhabiscam@gmail.com).

526 # Reference:

527 1. Liu D, Uzonna JE. The early interaction of Leishmania with macrophages and dendritic
528 cells and its influence on the host immune response. Front Cell Infect Microbiol [Internet].
529 2012 Jun 12 [cited 2025 Dec 5]; 2:83. Available from: www.frontiersin.org

530 2. Gregory DJ, Olivier M. Subversion of host cell signalling by the protozoan parasite
531 Leishmania. Parasitology [Internet]. 2005 Mar [cited 2025 Dec 5];130(S1):S27–35.
532 Available from: https://www.cambridge.org/core/journals/parasitology/article/subversion-
533 of-host-cell-signalling-by-the-protozoan-parasite-
534 leishmania/84909F03395390B2385B944C9A9A8FD2

535 3. Thakur L, Kushwaha HR, Negi A, Jain A, Jain M. Leptomonas seymouri Co-infection in
536 Cutaneous Leishmaniasis Cases Caused by Leishmania donovani From Himachal Pradesh,
537 India. Front Cell Infect Microbiol [Internet]. 2020 Jul 15 [cited 2025 Dec 5];10:550999.
538 Available from: www.frontiersin.org

539 4. Dixit KK, Ramesh V, Upadhyay S, Singh AK, Singh OP, Sundar S, et al. Utility of Blood
540 as the Clinical Specimen for the Molecular Diagnosis of Post-Kala-Azar Dermal
541 Leishmaniasis. J Clin Microbiol [Internet]. 2021 Aug 1 [cited 2025 Dec 5];59(9).
542 Available from: /doi/pdf/10.1128/jcm.00132-21?download=true

543 5. Ghosh S, Banerjee P, Sarkar A, Datta S, Chatterjee M. Coinfection of Leptomonas
544 seymouri and Leishmania donovani in Indian leishmaniasis. J Clin Microbiol [Internet].
545 2012 Aug [cited 2025 Dec 5];50(8):2774–8. Available from: /doi/pdf/10.1128/jcm.00966-
546 12?download=true

547 6. Selvapandiyan A, Ahuja K, Puri N, Krishnan A. Implications of co-infection of
548 Leptomonas in visceral leishmaniasis in India. Parasitology [Internet]. 2015 Oct 23 [cited
549 2025 Dec 5];142(14):1657–62. Available from:
550 https://www.cambridge.org/core/journals/parasitology/article/implications-of-coinfection-
551 of-leptomonas-in-visceral-leishmaniasis-in-
552 india/5A7C113DC9AA989F637AA5BB6DC08E00

553 7. Kraeva N, Butenko A, Hlaváčová J, Kostygov A, Myškova J, Grybchuk D, et al.
554 Leptomonas seymouri: Adaptations to the Dixenous Life Cycle Analyzed by Genome
555 Sequencing, Transcriptome Profiling and Co-infection with Leishmania donovani. PLoS
556 Pathog [Internet]. 2015 Aug 1 [cited 2025 Dec 5];11(8). Available from:
557 https://pubmed.ncbi.nlm.nih.gov/26317207/

558 8. Kutish GF, Janovy J. Inhibition of in vitro macrophage digestion capacity by infection
559 with Leishmania donovani (Protozoa: Kinetoplastida). Journal of Parasitology.
560 1981;67(4):457–62.

561 9. DO A. Macrophages as destructive cells in host defence. Inflammation : Basic Principles
562 and Clinical Correlates [Internet]. 1992 [cited 2025 Dec 5];637–62. Available from:
563 https://cir.nii.ac.jp/crid/1571980076173091968

564 10. Rossi M, Castiglioni P, Hartley MA, Eren RO, Prével F, Desponds C, et al. Type I
565 interferons induced by endogenous or exogenous viral infections promote metastasis and
566 relapse of leishmaniasis. Proceedings of the National Academy of Sciences [Internet].
567 2017 May 9 [cited 2026 Feb 10];114(19):4987–92. Available from:
568 /doi/pdf/10.1073/pnas.1621447114?download=true

569 11. Adaui V, Lye LF, Akopyants NS, Zimic M, Llanos-Cuentas A, Garcia L, et al.
570 Association of the endobiont double-Stranded RNA virus LRV1 with treatment failure for
571 human leishmaniasis caused by Leishmania braziliensis in Peru and Bolivia. Journal of
572 Infectious Diseases [Internet]. 2016 Jan 1 [cited 2026 Feb 10];213(1):112–21. Available
573 from: https://itg.elsevierpure.com/en/publications/association-of-the-endobiont-double-
574 stranded-rna-virus-lrv1-with-/

575 12. Lye LF, Akopyants NS, Dobson DE, Beverley SM. A Narnavirus-like element from the
576 trypanosomatid protozoan parasite Leptomonas seymouri. Genome Announc [Internet].
577 2016 [cited 2025 Dec 5];4(4):713–29. Available from: /doi/pdf/10.1128/genomea.00713-
578 16?download=true

579 13. Sukla S, Roy S, Sundar S, Biswas S. Leptomonas seymouri narna-like virus 1 and not
580 leishmaniaviruses detected in kala-azar samples from India. Archives of Virology 2017
581 162:12 [Internet]. 2017 Sep 22 [cited 2025 Dec 5];162(12):3827–35. Available from:
582 https://link.springer.com/article/10.1007/s00705-017-3559-y

583 14. Sukla S, Nath H, Kamran M, Ejazi SA, Ali N, Das P, et al. Detection of Leptomonas
584 seymouri narna-like virus in serum samples of visceral leishmaniasis patients and its

585 possible role in disease pathogenesis. Sci Rep [Internet]. 2022 Dec 1 [cited 2025 Dec
586 5];12(1). Available from: https://pubmed.ncbi.nlm.nih.gov/36002553/

587 15. Mirabedini Z, Mirjalali H, Kazemirad E, Khamesipour A, Samimirad K, Koosha M, et al.
588 The effects of Leishmania RNA virus 2 (LRV2) on the virulence factors of L. major and
589 pro-inflammatory biomarkers: an in vitro study on human monocyte cell line (THP-1).
590 BMC Microbiology 2023 23:1 [Internet]. 2023 Dec 14 [cited 2026 Feb 10];23(1):398-.
591 Available from: https://link.springer.com/article/10.1186/s12866-023-03140-0

592 16. Srivastava P, Prajapati VK, Vanaerschot M, Van der Auwera G, Dujardin JC, Sundar S.
593 Detection of Leptomonas sp. parasites in clinical isolates of Kala-azar patients from India.
594 Infection, Genetics and Evolution [Internet]. 2010 Oct 1 [cited 2025 Dec 5];10(7):1145–
595 50. Available from:
596 https://www.sciencedirect.com/science/article/pii/S1567134810001978

597 17. Pacheco RS, Marzochi MCA, Pires MQ, Brito CMM, Madeira MDF, Barbosa-Santos
598 EGO. Parasite Genotypically Related to a Monoxenous Trypanosomatid of Dog's Flea
599 Causing Opportunistic Infection in an HIV Positive Patient. Mem Inst Oswaldo Cruz
600 [Internet]. 1998 [cited 2025 Dec 5];93(4):531–7. Available from:
601 https://www.scielo.br/j/mioc/a/pNj7MJrzmngWJs48zDhWr5z/?lang=en

602

603

604

605

606 # Figure Legends

607

608 **Fig 1. Quantification of parasite load from infected macrophage cells.**

609 Parasite load was assessed in culture **(A)** supernatants and **(B)** cell lysates from parasite infected
610 RAW 264.7 cells at 48- and 168 h post-infection. Parasite load quantified from infected THP-1
611 macrophage **(C)** supernatants and **(D)** lysates at 48-,96- and 168- h.p.i. **(E)** Motile parasite counts
612 from transformation/subculture flasks at 12 days post-transfer, derived from infected
613 macrophage harvests collected at 48, 96, and 168 h.p.i and monitored using a hemocytometer.**(F)**
614 Approx. 10^7 parasites /well were maintained in DMEM-10 at 37 °C for 48-168h and
615 subsequently 2 x 10^6 parasites/time point were transferred to Schneider's medium at 22 °C to
616 assess revival capacity at different time points.**(G)** Representative ITS-1 PCR image from DNA
617 extracted from total parasite pellets harvested after exposure to macrophage growth conditions.
618 PCR amplicons were resolved on a 1% agarose gel. L1: Ladder; L2- L4: LD PCR bands from
619 parasites inoculated in DMEM-10 and totally pelleted after 24-, 72- and 168 h. L5-L7: LD PCR
620 bands from parasites inoculated in RPMI-10 for 24-, 72- and 168 h, L8: 10^6 LD DNA as positive
621 control; L9-L11: LS PCR bands from parasites inoculated in DMEM-10 and totally pelleted after
622 24-, 72- and 168 h. L12-L14: LS PCR bands from parasites inoculated in RPMI-10 and totally
623 pelleted after 24-, 72- and 168 h, L15: 10^6 LS DNA as positive control (where L represents Lane
624 number). (H) IL-12p40 cytokine level was measured by ELISA from cell supernatant infected
625 with LD, LS and co-culture at 72 h.p.i. For (A-F and H), the data were represented as mean ± SD
626 of a minimum of three independent experiments. Statistical comparisons were made using an
627 unpaired two-tailed Student's t-test or one way-Anova where $p < 0.05$ (*), $p < 0.01$ (**), $p <$
628 0.001 (***), $p < 0.0001$ (****), ns = non- significant.

629 **Fig 2. Quantification of viral load from parasite infected macrophage cells.**

630 Viral titres were assessed in culture **(A)** supernatants and cell lysates from parasite infected
631 RAW 264.7 cells at 48 h.p.i. Viral load quantified from infected RAW 264.7 macrophage. **(B)**
632 supernatants and **(C)** lysates at 48- and 168- h.p.i. Quantification of viral titres from culture. **(D)**
633 supernatants and **(E)** cell lysates of parasite infected THP-1 cells at 48-, 96- and 168 h.p.i.
634 representative images of semi nested RT-PCR analysis for detection of Lepsey NLV1 from virus
635 infected RAW 264.7 **(F)** supernatant and **(G)** lysate at 48-, 72- & 96 h.p.i. M: marker, L1-L6:
636 represents 1st round of PCR and L7-L12: represents 2nd round of PCR. L1 and L7: cell control,
637 L2-L4 and L8-L10: 48-72-96 h.p.i. samples respectively. L5 and L11: positive control, L6 and
638 L12: negative control (where L represents lane number). For (A-E), the data are represented as
639 mean ± SD of a minimum of three independent experiments. Statistical comparisons were made
640 using an unpaired two-tailed Student's t-test or one way-Anova where $p < 0.05$ (*), $p < 0.001$
641 (***), $p < 0.0001$ (****), ns = non-significant.

642

643 **Fig 3**: **Microscopic examination of Giemsa-stained infected macrophage cells**
644 **at 72 h.p.i.**

645 **(A)** uninfected RAW 264.7 macrophage cells; **(B)** RAW 264.7 macrophages infected with LD;
646 **(C)** RAW 264.7 macrophages infected with LS. **(D)** Uninfected THP-1 macrophage cells; **(E)**
647 THP-1 cells infected with LD; **(F)** THP-1 cells infected with LS. All images were acquired under
648 a light microscope at 1000× magnification. Scale bar: 10 µm.

649

650 **Fig 4**: **Schematic representation of parasite and viral load dynamics during**
651 **mono-infection and co-infection in murine and human macrophage models.**

652 # Supporting Information Legends

653

654 **S1 Table. Quantitative analysis of ITS1 qPCR-derived parasite load in RAW**
655 **264.7 cells.**

656 Parasite load was quantified from supernatant and lysate samples collected at 48 and 168 h post-
657 infection (h.p.i.). Data are presented as mean ± SD from a minimum of three independent
658 experiments.

659

660 **S2 Table. ImageJ-based relative band intensity analysis of ITS1 PCR products**
661 **from infected RAW 264.7 cells.**

662 Relative band intensities of ITS1 PCR products were quantified from supernatant and lysate
663 samples of parasite-infected RAW 264.7 cells at 48 and 168 h post-infection (h.p.i.).

664

665 **S3 Table. Quantitative analysis of parasite load from infected THP-1 cells.**

666 Parasite load was quantified from supernatant and lysate samples collected at 48, 96, and 168 h
667 post-infection (h.p.i.). Data are presented as mean ± SD from a minimum of three independent
668 experiments.

669

670 **S4 Table. ImageJ-based relative band intensity analysis of ITS1 PCR products**
671 **from parasite-infected THP-1 cells.**

672 Relative band intensity of ITS1 PCR products was analyzed from supernatant and lysate samples
673 of parasite-infected THP-1 cells at 48, 96, and 168 h post-infection (h.p.i.).

674 S5 Text. Supplementary microscopic enumeration of motile parasites and 675 corresponding graphical representation.

676 This file contains **(S5 Table)** showing representative counts of motile parasites per four
677 microscopic fields and **(S1 Fig)** showing graphical representation of the same data.
678

679 S6 Text. Microscopic enumeration of motile parasites and corresponding 680 graphical analysis at 11 days post-transfer.

681 This file contains **(S6 Table)** showing representative microscopic parasite counts from two
682 different fields and **(S2 Fig)** showing graphical representation of motile parasite counts.
683

684 S7 Table. Representative counts of motile and transformed parasites in 685 subculture flasks at different time points -12 days post-transfer.

686 Motile and transformed parasites were quantified using a haemocytometer following transfer of
687 harvested cells into subculture flasks at the indicated time points. Data are presented as mean ±
688 SD from a minimum of three independent experiments.

689

690 **S8 Text. Supplementary data showing viable and motile parasite counts and**
691 **graphical representation after subculture.**

692 This file contains **(S8 Table)** showing hemocytometer-based parasite counts and **(S3 Fig)**
693 showing graphical representation of parasite counts.

694

695 **S9 Table. Quantitative analysis of viral load in infected RAW 264.7**
696 **macrophages.**

697 Viral load was quantified from infected RAW 264.7 cell culture supernatant and cell lysate at 48
698 and 168 h post-infection (h.p.i.). Data are presented as mean ± SD from a minimum of three
699 independent experiments.

700

701 **S10 Table. Quantitative analysis of viral load in infected THP-1 macrophages.**

702 Viral load was quantified from infected THP-1 cell culture supernatant and cell lysate at 48, 96,
703 and 168 h post-infection (h.p.i.). Data are presented as mean ± SD from a minimum of three
704 independent experiments.

705

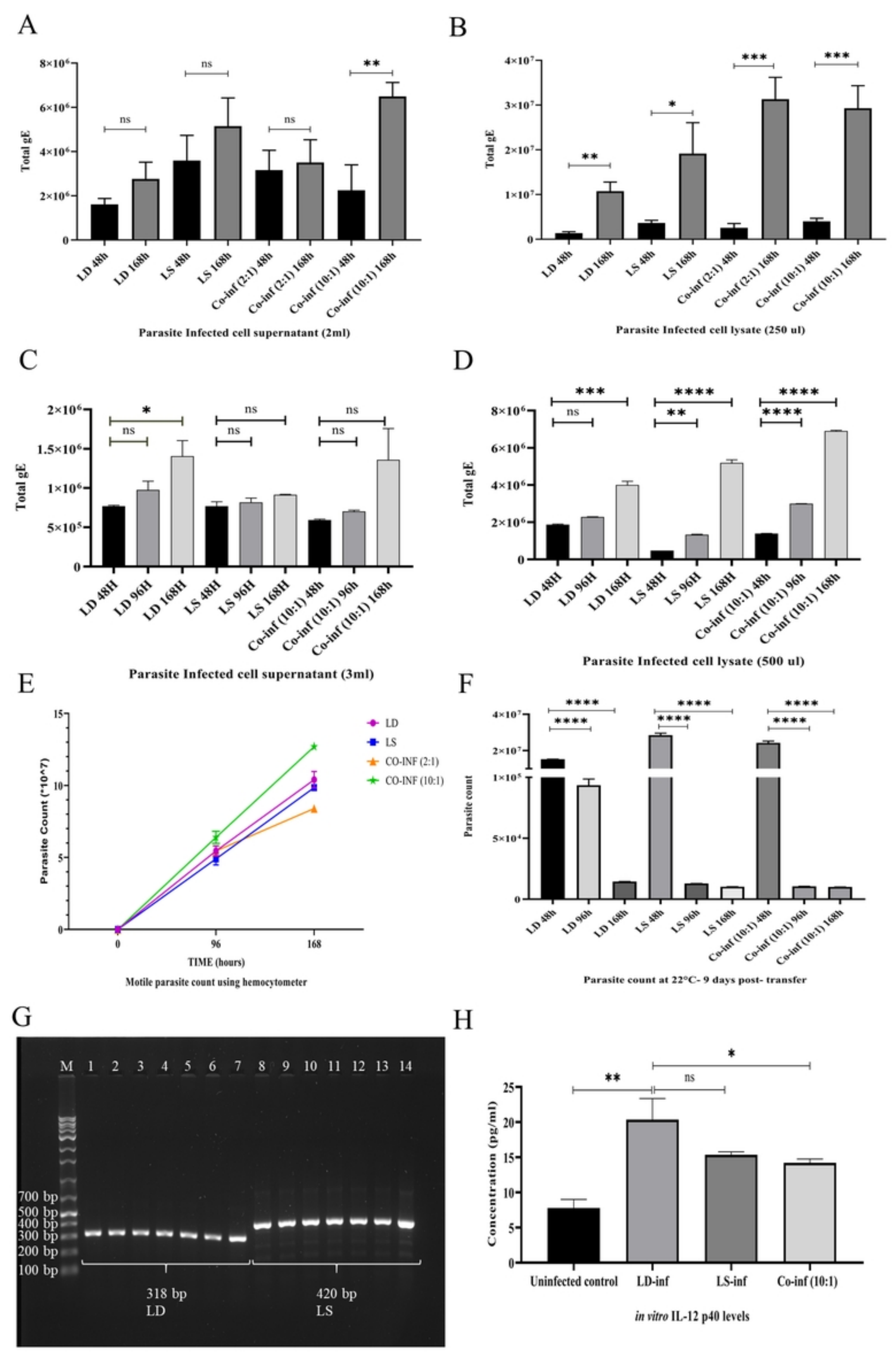
A
Total gE
Parasite Infected cell supernatant (2ml)
B
Total gE
Parasite Infected cell lysate (250 ul)
C
Total gE
Parasite Infected cell supernatant (3ml)
D
Total gE
Parasite Infected cell lysate (500 ul)
E
Parasite Count (*10^7)
TIME (hours)
Motile parasite count using hemocytometer
LD
LS
CO-INF (2:1)
CO-INF (10:1)
F
Parasite count
Parasite count at 22°C- 9 days post- transfer
G
M 1 2 3 4 5 6 7 8 9 10 11 12 13 14
700 bp
500 bp
400 bp
300 bp
200 bp
100 bp
318 bp
LD
420 bp
LS
H
Concentration (pg/ml)
Uninfected control
LD-inf
LS-inf
Co-inf (10:1)
in vitro IL-12 p40 levels

Figure 1

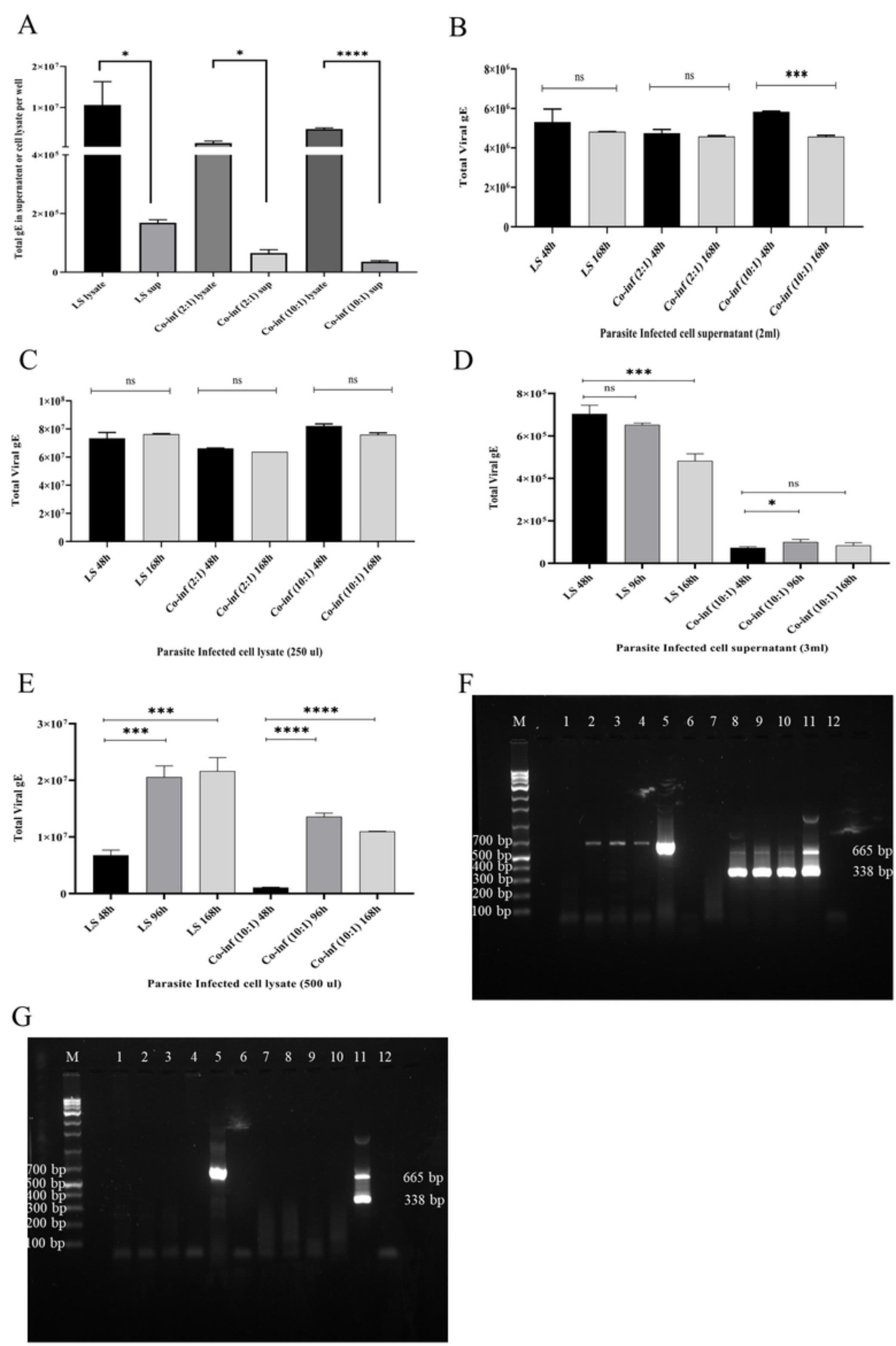
A
Total gE in supernatent or cell lysate per well
LS lysate
LS sup
Co-inf (2:1) lysate
Co-inf (2:1) sup
Co-inf (10:1) lysate
Co-inf (10:1) sup
B
Total Viral gE
LS 48h
LS 168h
Co-inf (2:1) 48h
Co-inf (2:1) 168h
Co-inf (10:1) 48h
Co-inf (10:1) 168h
Parasite Infected cell supernatant (2ml)
C
Total Viral gE
Parasite Infected cell lysate (250 ul)
D
Total Viral gE
LS 48h
LS 96h
LS 168h
Co-inf (10:1) 48h
Co-inf (10:1) 96h
Co-inf (10:1) 168h
Parasite Infected cell supernatant (3ml)
E
Total Viral gE
Parasite Infected cell lysate (500 ul)
F
M 1 2 3 4 5 6 7 8 9 10 11 12
700 bp
500 bp
400 bp
300 bp
200 bp
100 bp
665 bp
338 bp
G
M 1 2 3 4 5 6 7 8 9 10 11 12
700 bp
500 bp
400 bp
300 bp
200 bp
100 bp
665 bp
338 bp

Figure 2

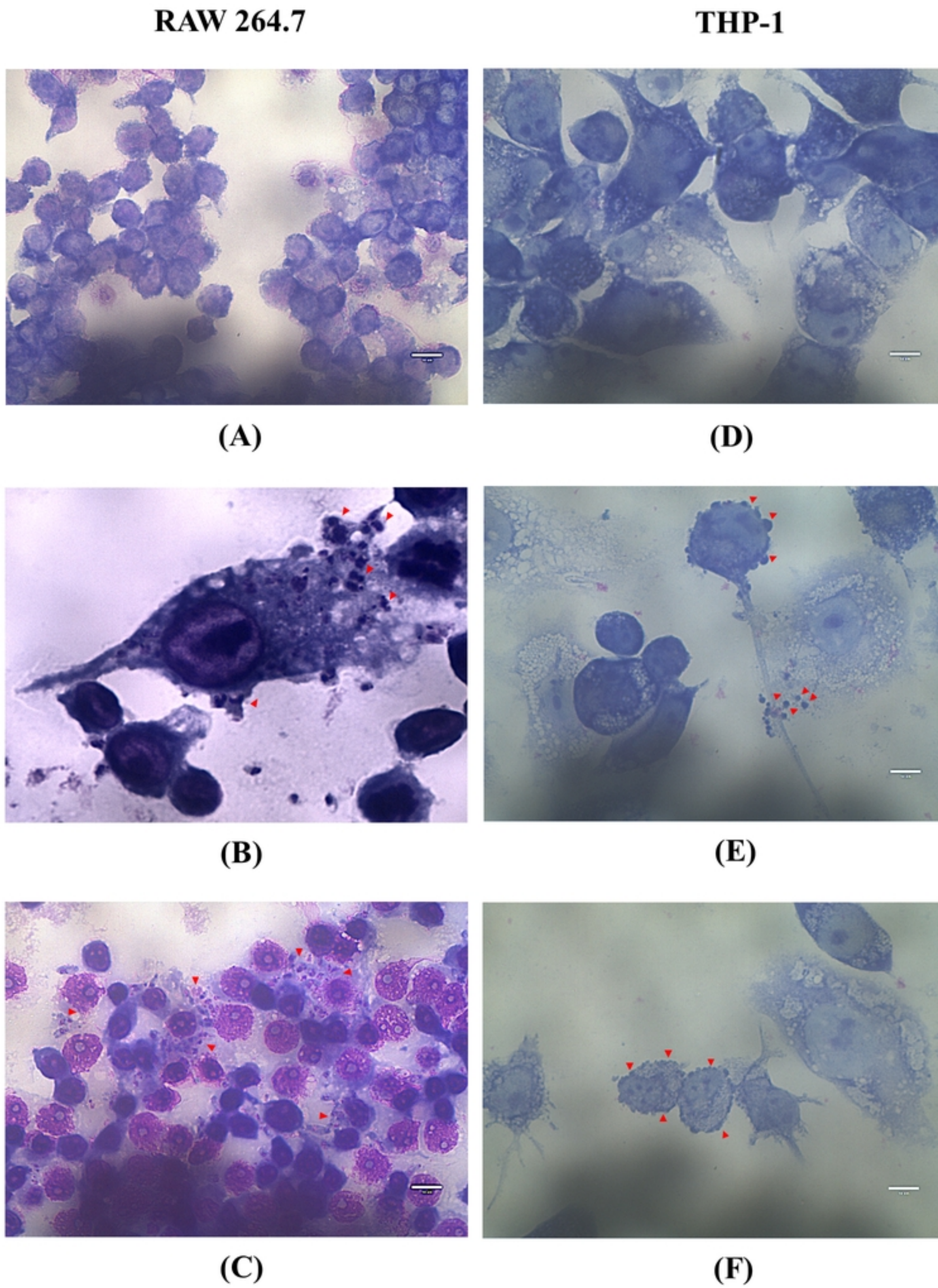

Figure 3

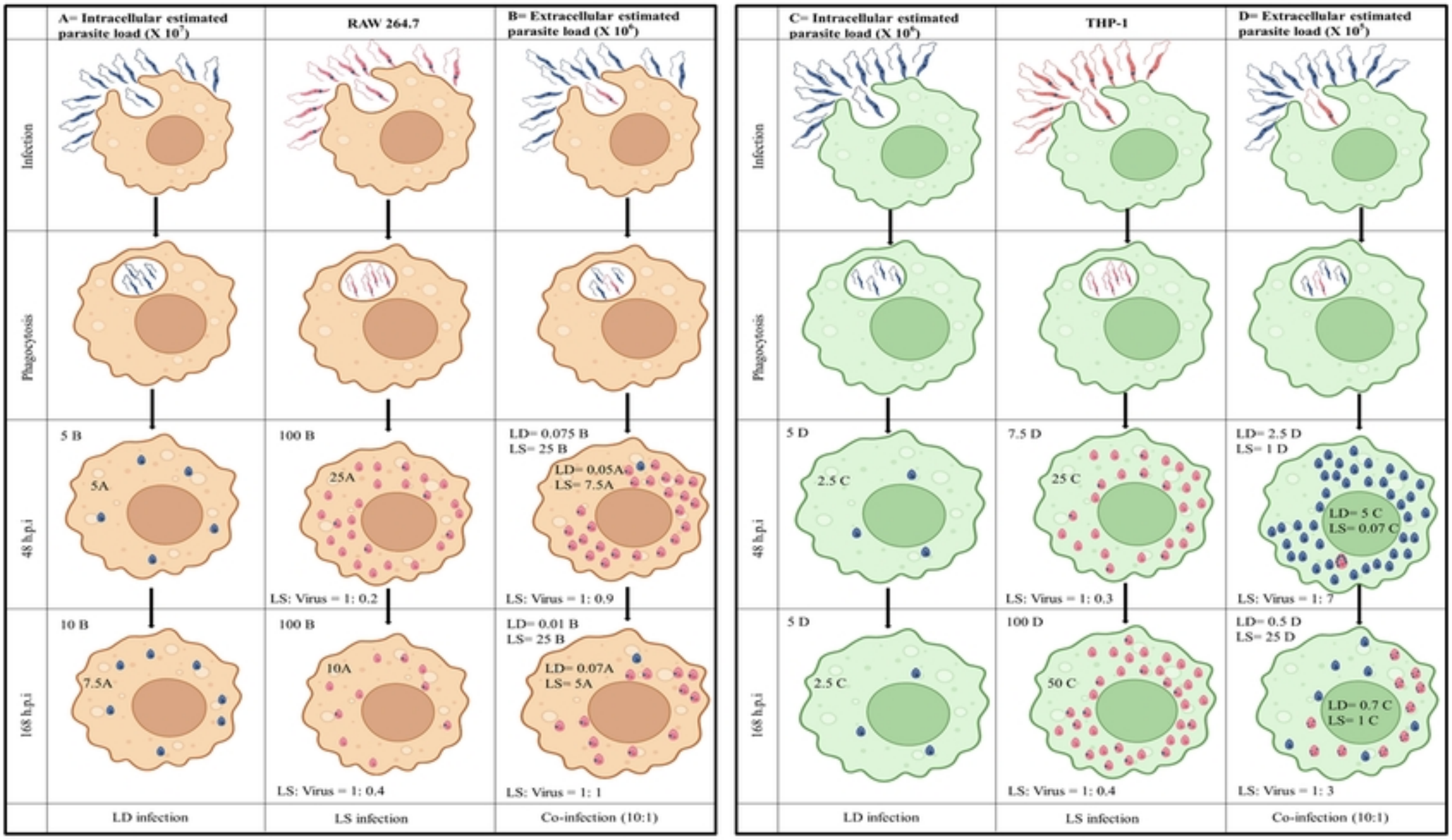

• Co-infection with LD **reduces host cell lysis** compared to mono-infection, thereby creating a more permissive intracellular environment that **supports LS persistence**.

• In co-infection scenario, the intracellular burden of virus increased compared to LS mono-infection,

- **RAW 264.7 macrophages: ~2.5–4.5-fold** increase in viral load.
- **THP-1 cells: ~7.5–23-fold** increase in viral load.
- **Enhanced intracellular viral survival or replication** in the presence of LD during co-infection.

* LD: LS relative quantity in co-infection was assayed by ImageJ analysis.

Figure 4